

Measurement of the Effective Sensitive Volume of FAMOS Cells of an Ultraviolet Erasable Programmable Read Only Memory

Leif Z. Scheick, Peter J. McNulty, *Senior Member, IEEE*, and David R. Roth

ABSTRACT--A method is described for measuring the sensitive volume of the oxide which makes up the collection region for erasure surrounding the floating gate of the FAMOS cell of a Ultraviolet erasable Programmable Read Only Memory (UVPROM) using the data acquired from the output of the pins of the device. A direct measurement of the dose required to erase the Floating gate Avalanche injected Metal Oxide Silicon (FAMOS) cell yields a measurement of the volume of oxide which collects the charge. Another method using target theory to determine the sensitive volume of the device is also presented with good agreement between the methods. The sensitive volume depends on the LET of the radiation. The ramifications for microdosimetry and cell failure are discussed as well as for the long term use aspects of non-volatile memories.

I. INTRODUCTION

With a large number of long term space missions being flown with non-volatile memory (NVM) banks as integral avionics systems, such as the upcoming mission to Europa, the need to precisely understand the effects of radiation on the NVM types has grown considerably. This is mostly because the NVM banks on such missions are by far the most susceptible to total ionizing dose (TID) effects, and fairly susceptible to single event effects (SEE) [1]. The variation of radiation effects with variables like dose rate, LET, and radiation type has become very important. The UVPROM allows easy investigation into some radiation effects on NVMs.

A UVPROM stores information on a floating gate. The floating gate's charge determines the digital state of the cell. The structure of the UVPROM's cell is similar to other NVMs, like the EEPROM or flash memories. UVPROMs are erased by exposure to radiation [2]. Electron-hole pairs are generated in all areas of the circuit when ionizing radiation interacts with microelectronic circuits [3]. In the FAMOS cell

of a UVPROM, some of the holes may interact with the floating gate of the cell to reduce its stored charge [2], [3]. The reduced charge allows measurements of absorbed dose [4]. Electrons may also be removed from the gate by direct radiation interaction. Several floating gate designs and devices have been studied in terms of radiation response [4]-[10].

In this study, various methods of determining the amount of erasure of the floating gate as a function of dose. The parameters that describe the erasure have been shown to change with radiation type and more probably LET [4], [11]. This paper describes a procedure for estimating the sensitive volume of the oxide which makes up the collection region for erasure surrounding the floating gate of the FAMOS cell. The parameter used is the dose required to remove a certain amount of charge from the floating gate of a UVPROM.

II. THEORY AND EXPERIMENT

The structure of the FAMOS cell is similar to a standard FET except for a small conductor, called the floating gate, which is imbedded in the oxide between the control gate and the conduction channel of the device. The FAMOS transistor is used as a NVM cell by injecting charge onto the floating gate. Hot electrons transport through the insulating oxide onto the floating gate due to a large electric field from the control gate. The floating gate repels any further injected charge when the charge on the floating gate is saturated. Maximum charge is reached when the field, due to the floating gate, is approximately equal to the injection field.

A memory state is determined by whether the floating gate is charged or left uncharged in programming. The channel will or will not conduct when the read voltage (5V) is applied to the control gate depending on whether or not the floating gate is programmed. A loaded floating gate then presents a negative bias to the channel, making the FET non-conducting even when there is a positive voltage on the control gate. This turns off the FET. The band diagram of such a device is shown in Fig. 1 [12], [13].

Manuscript received July 23, 2000. The research in this paper was carried out in part by the Jet Propulsion Laboratory, California Institute of Technology, under contract with the National Aeronautics and Space Administration.

L. Z. Scheick is with the Jet Propulsion Laboratory, California Institute of Technology, Pasadena, Ca, 91109 USA (telephone: 818-354-3272, e-mail: leif.scheick@jpl.nasa.gov).

P. J. McNulty is with the Dept. of Physics and Astronomy, Clemson University, Clemson, SC 29634-1911 USA (telephone: 864-656-3416, e-mail: mpeter@clemson.edu).

D. R. Roth is with the Applied Physics Lab, Johns Hopkins University, Laurel, MD 20723-6099, USA (telephone: 443-778-4022, e-mail: David.Roth@jhuapl.edu).

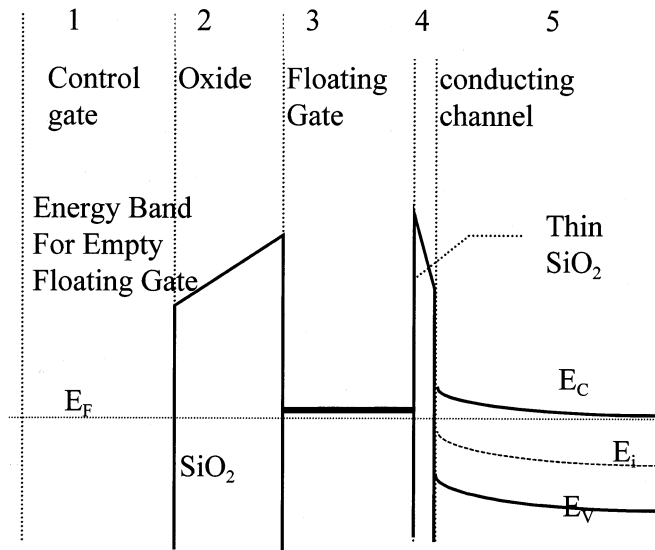


Fig. 1. A FAMOS transistor energy band diagram. The floating gate stores charge so the device can power down and still retain data. Ionizing radiation removes charge from the floating gate (area 3) by direct ionization or by creating holes in the oxide (areas 2 and 4) which drift to the floating gate and combine with a floating gate electron. This figure is not to scale.

Current will flow in the channel if the floating gate is not programmed since electrons may populate the channel. This is called the “conducting” state of the FET. Likewise, the “non-conducting” state occurs when there is charge on the floating gate, which depopulates the channel of electrons. The charge remaining on the floating gate is a function of absorbed dose since exposure to ionizing radiation gradually reduces the charge on the floating gate. When enough charge has been removed, the transistor changes from the non-conducting to the conducting state. Since the process is not instantaneous, the number of cell erasures, also called flips, as a function of exposure to normal UV is a gradual change [4]. All UV light used in this study has a wavelength of 254 nm.

A typical erasure response of the UVPROM to radiation is shown in Fig. 2. This structure is called an “S” curve. Also in Fig. 2 is the target theory fit of the data to the device. The target theory fit has been shown to be the response that best describes the data on experimental and theoretical grounds [11], [14], [15]. The reason that target theory is the obvious model for the erasure of the UVPROM is the similarity of the FAMOS cells to biological cells. The erasure of a FAMOS cell and the death of a biological cell both occur over multiple radiation hits. Each one of these hits neutralizes one or more targets on the cell. These are electrons for the floating gate. Single hit target theory, which is used throughout this study, is the multiplication of D number of target inactivations which are give by a simple exponential probability of erasure, or:

$$F_{tt}(t) = \left(1 - e^{-\frac{dose}{C}}\right)^D, \quad (1)$$

where dose represents the duration or amount of exposure. C and D are parameters of the model [4]. Specifically, D is the number of targets in the system and C is dose required to inactivate 63% of the members of the system given that D=1.

C and D can be estimated from the curve in Fig. 2. Also, the amount of radiation required to completely erase the device can be measured, which just the dose require to cause all bit is the UVPROM memory to report erasure.

The slight deviation of the data from the target theory fit is due to manufacture variances, UV radiation non-uniformity from the source, and variance in the quartz window. Removing the quartz window exacerbates the problem since the window focuses the UV light. The deviation does not effect the calculations.

An energetic charged particle generates electron-hole pairs according to its LET, and the amount of charge removed from the floating gate depends on the LET and the proximity of the trajectory to the gate. One would expect different radiation types to have similar but not identical effects because of different recombination rates and mechanisms [4], [12-19]. The parameters that determine the target theory curve should reflect this varying erasure in the data shown in Fig. 2. These parameters are what allow the measurement of the sensitive volume of the FAMOS cell. Many oxides and interfaces with structure similar to this have been studied [20]-[24].

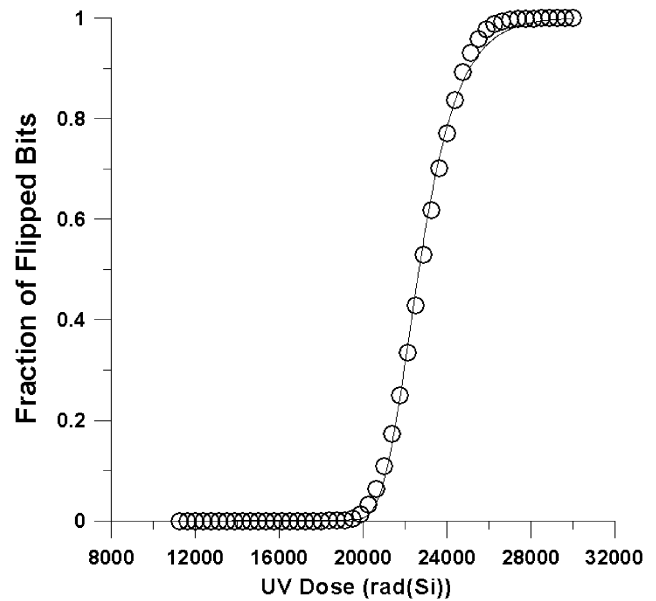


Fig. 2. The fraction of memory states to flip (0 to 1) as a function of the duration of exposure to UV radiation at an intensity of $50 \mu\text{W cm}^{-2}$. The fit to target theory is not perfect due to manufacture variance and UV flux variance. Target theory has been shown to be the distribution that best describes the data.

To be used as a dosimeter, the device is programmed per manufacturer instructions. The effect of any exposure to ionizing radiation is the partial removal of charge from the floating gate. This, in turn, reflects the amount of exposure received. The goal is to obtain curves like Fig. 2 for various radiation types. From these curves estimates of the target theory parameters and the dose required to erase all bits and be extracted. From these measurements, the sensitive volume of the oxide which makes up the collection region for erasure surrounding the floating gate of the FAMOS cell can be determined.

III. PROCEDURE AND SETUP

The devices used in this study were AMD27C64 series UVPROMs consisting of 65,536 FAMOS cells in an 8192x8 bit format. UV radiation can erase the device in part due to a quartz lens encased in the ceramic dip directly over the cells. The normal commercial use of this device is as a read only memory. The UVPROM is exposed to low energy (<8 eV) ultraviolet radiation, which removes electrons from the floating gate, if erasure is desired.

There are three methods used in determining the erasure distributions. All three types are passive since power is removed during irradiation. The first method, called the live readout method, is the direct reading of the number of erasures as a function of applied radiation. The DUT is readout between bursts of radiation at accelerators or other sources to determine number of flips as a function of dose. Radiation can be of any type, including UV, proton, and heavy ion. This is unlike previous readout methods in that it does not require UV to estimate erasure.

The second and third methods are both remote methods, i.e., these methods prepare a device, then device is conveyed to a radiation source after which it is conveyed back to a laboratory to be readout. Basically, in the second method, dose measurements correlate with the difference in time to erase a device with UV between a programmed device and a programmed then irradiated device. The procedure of an ionizing radiation exposure that of is several "pre-runs" to determine the time required to erase each bit by exposure to UV. A programmed device is then irradiated, and then the required time to erase each bit using UV is measured. The change in the time to erase the device in a "pre-run" and run right after irradiation correlates to dose. To determine residual effects, such as SEGR or severe oxide effects, etc., the device is subjected to several "post-runs" which are identical to the pre-runs. A more in-depth description of how this method works is provided in [4], [11]. This method is called the remote time shift method.

The final method can make small (~5 rad(Si)) measurements over the widest dynamic range. As can be seen in Fig. 2, a UVPROM will absorb over half of the dose required to erase the device before any of the bits flip. Any small dose measurement would have to be made when the device is partially erased enough to be in the sloped region (20 to 30 krad(Si) in Fig. 2). To guarantee that at least one part of the device is optimally sensitive to small dose changes, the UVPROM memory is divided into small sections. For a 65,536-bit device, eight 8,192-bit sections are used. Each section is programmed and exposed to a different amount of UV. This procedure guarantees that at least one section will immediately report errors after exposure to radiation. Large doses are measured by the change in sections that have been totally erased, while small doses are measured by analyzing the changes in the amount that the current section has erased. This method has the advantage of not requiring any UV after preparation steps. Outlined in more detail in [4], [11], this is called the remote threshold shift method. The remote time

shift method and the remote threshold shift method have been shown to be equivalent [4], [11]. Both remote methods measure dose in equivalent seconds of UV radiation.

Table I illustrates a comparison of these methods. The "Optimum efficiency" column is a measure of how well the method acquires data. The unit of cycles is defined as the number of device interrogations required to yield one dose measurement. The "Optimum precision" column is an indicator of the minimum measurement of how small a measurement can be at optimal conditions. The "Dynamic range" column depends on radiation type, so the values in Table I are general ranges. It is important to note that all three methods are passive, i.e., the device is powered down during irradiation. Currently, a method of actively reading out the device during ion irradiation has been unsuccessful due to apparent burnout and gate ruptures in the device. This effect is currently under investigation.

The UVPROM exhibits a predictable UV dose rate response, so great care was taken to ensure that all UV based measurements and comparisons used the same UV response characteristics. The change in device response with temperature is known to be very slight. All devices were maintained at approximately 25 °C for all experiments and small thermal deviations do not affect measurements.

TABLE I
COMPARISON OF PASSIVE READOUT METHODS.

Type of Readout	Read Mode	Optimum Efficiency [cycles]	Optimum Precision [rad(Si)]	Dynamic Range [rad(Si)]
Live	Passive	10^7	5	10^3 - 10^5
Remote time shift	Passive	10^8	10^3	10^3 - 10^5
Remote threshold shift	Passive	10^9	5	5 - 10^5

A. Equivalent Electron LET

Electrons and high-energy photons present a unique problem in using electron radiation in these experiments. Due to their small mass in comparison with heavy particles, the LET of the particle is smaller on average and the interaction is quite different. The most probable interaction for electrons is the transfer of a significant fraction of energy to electrons at atomic positions. The initial scattered electrons can reach a very high energy level, and they will induce additional scattering events. A penetration of a few millimeters into the medium will result in a cascade of secondary electrons. These electrons can go on to produce electron-hole pairs or liberate electrons from the floating gate or depletion regions [25]. Though the details of this phenomenon remain unresolved, approximations can be made [26]. Research is currently being conducted to determine measurements that quantify the way in which electrons and generated secondary electrons deposit energy in matter. Radiobiological and medical measurements of electron dose are very exact [27]. In the application of most electron dosimetry methods, virtual water is placed in front of

the target to measure tissue equivalent dose. Most of the energy deposition is due to secondary electron production.

The effects of the energy depth dependence of electron radiation in matter are well known [28]. After a few millimeters of penetration into the target, the energy spectrum of electron energy ranges from zero to that of the incident electrons. Therefore, the LET values of electrons are not as well defined. Since a large fraction of the dose is due to slower electrons, the effective LET should be higher. Because of the scattering of electrons, the recombination nature of saturated oxide, and the higher LET of electrons that will be stopped near the floating gate, the LET in the oxide around the floating gate can be as much as three orders of magnitude higher than the incident energy of the primary electron.

A simple calculation can show this. Since the electron energies of interest are approximately 1000 eV to 1 MeV, the LET of an electron is approximately

$$LET(Q) = \frac{LET_0 E_0}{Q}, \quad (2)$$

where LET_0 and E_0 are reference values and Q is the electron energy. The goal here is the amount of energy deposited per unit length, parallel to the path of the primary, due to the primary and all of the secondary electrons after saturation has occurred. The fact that the electrons scatter forward means that the secondary electrons will deposit more energy per unit length than the forward moving primary, which in turn means that the angle of scatter will adjust the stopping power by a weighting factor of $\frac{1}{\cos(\mathbf{q})}$ where \mathbf{q} is the scattering angle.

The number of secondary electrons produced by the primary per scattered energy Q is [29]

$$N = \frac{\sqrt{E_0}}{\sqrt{Q}}, \quad (3)$$

and the energy as a function of scattering angle is [30]

$$Q = Ei \cos^2(\mathbf{q}). \quad (4)$$

where Ei is the incident particle energy. So the total energy deposited should be the product of (1), (2) and the weighting factor. Expressed mathematically:

$$LET_{eff}(Q) = \frac{LET_0}{\cos(\mathbf{q})} \left(\frac{E_0}{Q} \right)^{3/2}. \quad (5)$$

The energy deposited over all secondary energies is the goal, so using (4) to remove the Q variable and to good approximation setting $Ei=E_0$, the result is

$$LET_{eff} = \frac{LET_0}{\cos^4(\mathbf{q})}. \quad (6)$$

The maximum Q is half Ei and the minimum Q is 1000 eV. This correlates to integration limits of 45 to 85 degree. The resulting integration of (6) yields

$$LET_{eff} \approx 10^3 LET_0. \quad (7)$$

This is a somewhat simplistic calculation but it shows the importance of the secondary electron radiation in the system. Since the primary electron energies used in this study are in the MeV range, this approximation is valid. It is important to note that (7) does not imply that energy is created or the primary electron has a higher LET in the FAMOS cell. Equation (7) was derived to show that due to the extreme forward scattering nature of electrons, the number of electron hole pairs in the oxide should give the impression of higher LET particles.

IV. RESULTS

A. Live Vs. Remote Readout Equivalency

The live readout methods described above should be equivalent to the other passive method used in this and previous studies [4], [11]. To show equivalency, an experiment was performed using protons. A curve similar to that in Fig. 2 was obtained for UV and protons. The results of these two parametric equations were plotted in Fig. 3. The relation is a power law of exponent 0.8, which is identical to results from both remote methods. Recovery of this effect is important since the three methods are used interchangeably in this study and in real world dosimetry application like MPTB [11].

The slight non-linearity in Fig. 3 is due to the lack of homogeneity in the UV radiated onto the device. This figure illustrates the importance and liability of UV in this process. Methods of removing UV from the process to obtain increased accuracy are under study.

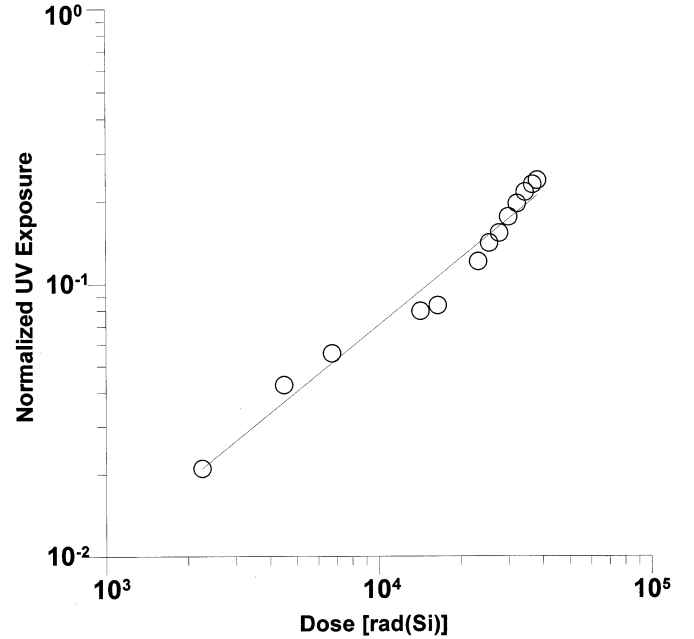


Fig. 3. The power law erasure response of the device to 50 MeV proton radiation. The results of live UV and proton irradiation parametrically plotted for the same amount of erasure. The deviation in the line is due to inhomogeneous UV. The exponent of the power law is 0.8, and it agrees well with the remote readout response. The exponent of the power law depends on the radiation type.

B. Readout Results

The plots the fraction of cell erasures as a function of doses for various radiation types are shown in Figs. 4 and 5. Fig. 4 shows the result of selected live readout methods. Shown are UV, 50 MeV protons and 1 GeV Argon ions. These erasure curves were directly measured during experiments at accelerators.

Fig. 5 illustrates "S" curves of selected remote methods conversion. These S curves are obtained by transforming the abscissa values of standard S curve from seconds of UV to rad(Si), i.e., the "P" curve is the "U" curve transformed by using the power law relations like the one shown in Fig. 3.

These curves, shown in Figs. 4 and 5, are all described by target theory relations and can be analyzed to determine the target theory parameters as well as the dose required for the complete erasure of the device for each radiation type. C and D in (1) can be estimated from the curves in Fig. 4 and 5. Also, the amount of radiation required to completely erase the device can be measured. These values are summarized in Table II when applicable. The power law behavior is most likely due to varying sensitivity to dose as a function of dose. The field of the floating gate will decrease with dose, which

leads to an exponential relationship, i.e., $E = E_0 e^{-\frac{Dose}{Dose_0}}$, where E_0 is the initial field and $Dose_0$ is a constant. This may explain why higher LET particles are less effective at erasing the device. So there must be two new erasure mechanisms that are shown here. The rate of erasure is based on dose and also LET, revealing that the oxide around the floating gate must contribute to the erasure mechanism. It is impossible to differentiate between these effects using only the output from the pins of the device.

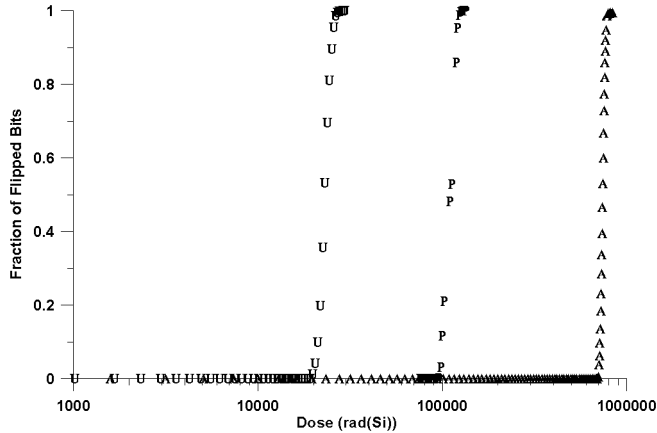


Fig. 4. The live readout erasure response of the device to various radiation types. The U point protector is UV, the P is 50 MeV protons, and A is 1 GeV Argon ions. The UV curve is based in part on the dose estimate from the erasure time and intensity specified by the manufacturer.

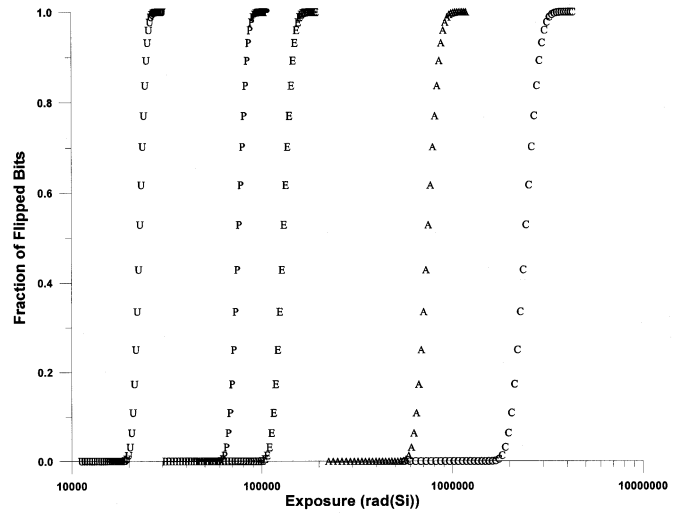


Fig. 5. The remote readout erasure response of the device to various radiation types. The U point protector is UV, the P is protons, the E is electrons, the A is Argon ions, and C is the Chlorine ions. The UV curve is based in part on the dose estimate from the erasure time and intensity specified by the manufacturer. These curves are generated by using the power-law relation of erasure due to irradiation and erasure to UV to transform the UV curve as a prototype.

TABLE II
THE PARAMETERS OF THE VARIOUS RADIATION SPECIES.

Radiation Type	Erasure Method ^a	LET [MeVcm ² /mg]	Exp. Power	Site ^b	C [rad (Si)]	D _{sat} [krad (Si)]
Proton	Live	0.003	N/A	IUCF	9458.92	135
Proton	Thresh	0.003	0.75	IUCF	N/A	116
Proton	Thresh	0.005	0.79	IUCF	N/A	125
Proton	Thresh	0.01	0.78	UCD	5968.05	107
Proton	Live	0.01	0.81	UCD	N/A	132
Electron	Thresh	2.511	0.69	GMH	11698.9	247
Electron	Thresh	2.511	0.70	GMH	N/A	227
Electron	Thresh	1.813	0.74	GMH	N/A	192
Electron	Time	2.511	0.71	GMH	N/A	265
6 MeV	Thresh	N/A	0.70	GMH	N/A	225
Photons						
Neon	Time	1.79	0.74	TAM	15133.4	193
Argon	Live	5.4	N/A	TAM	22328.8	795
Argon	Time	5.4	0.63	TAM	83685.6	1050
Chlorine	Thresh	11.4	0.5	BNL	310101	4259

^a Live is the live read method. Thresh is the remote threshold shift readout method. Time is the remote time shift method.

^b IUCF is the Indiana Cyclotron Facility. UCD is the UC Davis facility. GMH is the electron accelerator at Greenville Memorial Hospital. TAM is Texas A&M. BNL is Brookhaven National Lab.

C. Sensitive volume Calculation

The dependence of the exponent of the power law on the particle type conflicts with the assumption that the erasure of the gate should be linear with dose and independent of LET. The total-dose measurements indicate that the erasure is a power law of dose with respect to UV radiation as a standard, and particle LET does have an effect. Many studies on the effects of particle type on Si-SiO₂ interfaces have been done [31]. The conclusion of these studies is that LET is an issue in oxide structures. The LET is a measure of the local energy deposition due to the particle. Higher LET particles can also

induce spallation, recoil, and NIEL (Non-Ionizing Energy Loss) damage. So, the non-linear effect could be due to a wide variety of effects. Selected exposures of the dose required to erase plotted against the LET of the particle are shown in Fig. 6. The horizontal error bars on these graphs are due to the variation in the estimate of the LET of electrons. The vertical error bars are derived from Poisson counting statistics. There is a spread at the lowest LETs, which are the LETs for the protons. The spread results from noise.

An interesting question is then raised about whether or not this device can be used as a LET spectrometer. Certainly there is a LET dependence effect, but since the device requires 10^8 particles per square centimeter to make a measurement, this would be prohibitive for practical LET measurements.

By looking at the relationship in Fig. 6, one can start to see how much the oxide affects the erasure process. The relationship is an exponential dependence of erasure efficiency on LET. Not surprisingly, higher LET radiation experiences higher recombination and thus erasure rates are affected. A more obvious statement of this can be seen through the calculation of the effective sensitive volume thickness. Starting with an estimate of the total area of the cell:

$$A_{cell} = \frac{2mm^2}{65536} = 31m^2, \quad (8)$$

where $2 mm^2$ is the measured area of all 65536 FAMOS cells. Now, a good estimate of floating gate size is $A_{FG} = A_{cell}/10 = 3.1m^2$ [12], [13]. So the effective thickness of the oxide surrounding the floating gate should be

$$t_{eff} = \frac{V_{eff}}{A_{FG}} \quad \text{where } V_{eff} \text{ is volume of oxide around the}$$

floating gate that collects the energy that leads to the erasure of the floating gate. The sensitive volume can be found by calculating the energy required to completely erase the device:

$$E_{sat} = D_{sat} m_{sv} = D_{sat} rV_{eff}, \quad (9)$$

where D_{sat} is the dose required to erase the device, r is the density of the oxide, and m_{sv} is the mass of the sensitive volume. This is equal to the amount of energy required to generate enough holes in the oxide to remove the 10^4 electrons from the floating gate which will change the channel conductance enough to cause a bit flip to be reported [12], [13] or:

$$E_{sat} = 10^4 * 18eV. \quad (10)$$

By equating equations 9 and 10, then solving for V_{eff} , then

$$\text{plugging this value into } t_{eff} = \frac{V_{eff}}{A_{FG}} \text{ gives the effective}$$

thickness of the sensitive volume around the floating gate gives:

$$t_{eff} = \frac{1.8 * 10^5 eV}{rD_{sat} A_{FG}}. \quad (11)$$

The relationship between t_{eff} and LET is shown in Fig. 7.

The relationship is again exponential, revealing that the effective thickness of the collecting oxide decreases with increasing LET. The reason for this inverse effect may be due to the charge generation profile of higher LET particles.

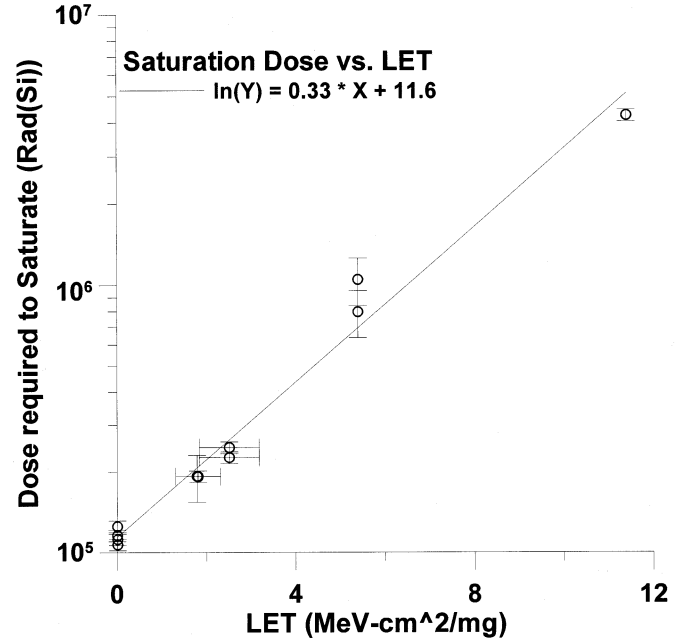


Fig. 6. Total dose required to erase the device versus LET of various radiation. The vertical error bars reflect Poisson counting statistics. The horizontal error bars reflect variation in LET estimates.

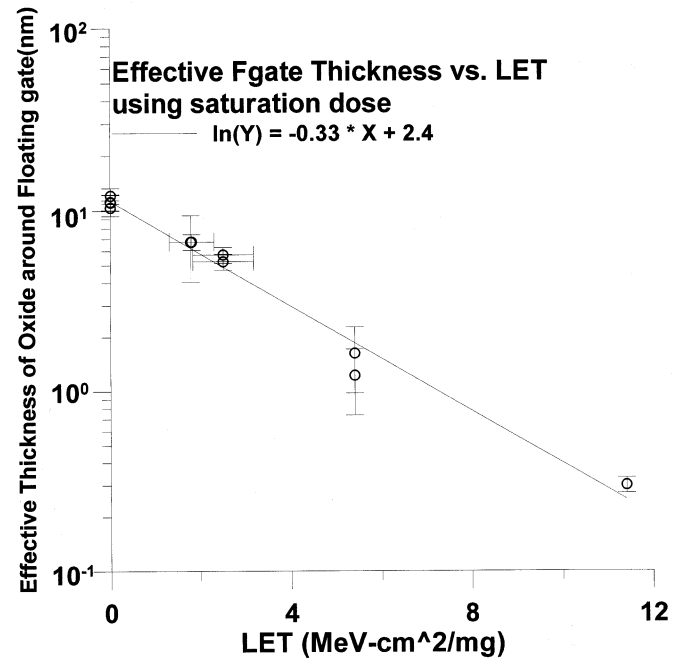


Fig. 7. Estimated sensitive volume thickness using the dose required to erase the device. The vertical error bars reflect Poisson counting statistics. The horizontal error bars reflect variation in LET estimates.

Target theory may also be used to determine the effective thickness of the sensitive oxide around the floating gate. As shown before, two parameters, C and D, uniquely determine the target theory model, which is shown in (1). C is the inverse of the sensitivity to erasure and D is the number of targets in the system. For a standard S curve, Fig. 2 for example, the C and D curve estimate how the device erases for a known flux. The parameters C and D can be estimated from these curves. These are plotted as a function of LET in Fig. 8. C increases with LET which shows that the target size decreases with LET. The effect of radiation on the D parameter is pursued in another study [32].

The C values obtained directly from the S curve yield the sensitive volume. The C value is the amount of radiation needed to flip 63% of the cells given that D=1. The condition of D equaling one means that the removal of one electron should cause the flip of the cell. Thus 63% of 65,536 of the cells should flip give C amount of dose, or 41288 for the whole die under the D=1 condition. Or:

$$E_{sat} = 41228 * 18eV. \quad (12)$$

So an electron hole pair should be created for this number of electrons. So equating equations 9 and 12, and using

$$t_{eff} = \frac{V_{eff}}{A_{FG}},$$

results in the following equation that may be used to determine the thickness of the sensitive volume:

$$t_{eff} = \frac{7.4 * 10^5 eV}{rCA_{AR}}. \quad (13).$$

where r is the density of the oxide around the floating gate and A_{AR} is area of the all of the gates which was 10% of 2 mm² or 0.2 mm² [12], [13]. Fig. 9 illustrates this dependence on LET.

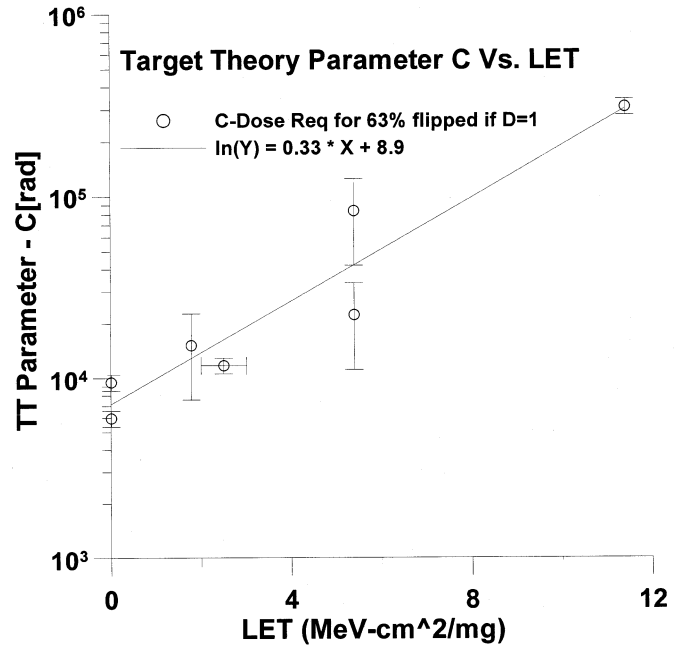


Fig. 8. Target theory parameter, C, versus LET of various radiation. The vertical error bars reflect Poisson counting statistics. The horizontal error bars reflect variation in LET estimates.

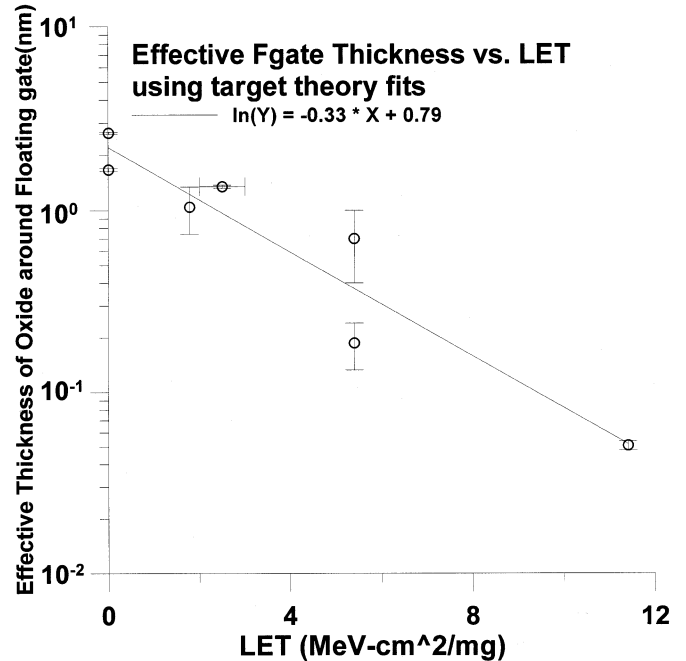


Fig. 9. Estimated sensitive volume thickness using the target theory parameter, C. The vertical error bars reflect Poisson counting statistics. The horizontal error bars reflect variation in LET estimates.

The results have the same decreasing exponential trend with the same exponential coefficient. The two curves differ by a factor of approximately 4.5, which is good agreement considering the assumptions made for both calculations.

It is important to remember that, since the erasure is not linear with dose, these effective thickness measurements are average thickness estimates. The power law relation between dose and erasure implies that the effective thickness will not be constant throughout erasure. The current measurements of

effective oxide thickness are order of magnitude estimates only, since several of the physical parameters were estimated. More detailed investigations are underway.

V. CONCLUSIONS

A new sensitive volume measurement approach using FAMOS FETs has been developed. Ionizing radiation neutralizes the charge on the floating gates that can be measured through the pins of a commercial UVPRM.

This method should work with any circuit that shows an increased effect with dose. The accrual of dose effects will follow can be modeled after arguments similar to target theory.

VI. ACKNOWLEDGMENTS

The research in this paper was carried out in part by the Jet Propulsion Laboratory, California Institute of Technology, under contract with the National Aeronautics and Space Administration.

VII. REFERENCES

- [1] H. Schwartz, D. Nichols, and A. Johnston, "Single-event upset in flash memories," *IEEE Trans. Nucl. Sci.*, vol. 44, no. 6, pp. 2315-2324 1998.
- [2] B. Prince and G. Due-Gundersen, *Semiconductor Memories*, New York: John Wiley and Sons, 1983.
- [3] E. Nicollian and J. Brews, *MOS Physics and Technology*, New York: John Wiley and Sons, 1982.
- [4] L. Scheick, P. McNulty, and D. Roth, "Dosimetry based on the erasure of the floating gates in the natural radiation environments in space," *IEEE Trans. Nucl. Sci.*, vol. 45, no. 6, pp. 2681-2688, 1998.
- [5] N. Tarr, G. Mackay, K. Shortt, and I. Thomson, "A floating gate dosimeter requiring no external power supply," *IEEE Trans. Nucl. Sci.*, vol. 45, no. 6, pp. 1470-1474, 1998.
- [6] J. Kassabov, N. Nedev, and N. Smirnov, "Radiation dosimeter based on floating gate transistors," *Radiation Effects and Defects in Solids*, vol. 166, 155-160, 1991.
- [7] J. Kahilainen, "The direct ion storage dosimeter," *Radiation Protection Dosimetry 1996*, vol. 66, 459-464, (1996).
- [8] D. Peters, N. Tarr, K. Shortt, I. Thompson, and G. Mackay, "A floating gate MOSFET gamma dosimeter," *Can. J. Phys.*, vol. 74, pp. 135-140, 1996.
- [9] Patent number 5,961,699.
- [10] A. Kelleher, N. McDonnell, B. O'Neil, W. Lane and L. Adams, "Investigation into the reuse of PMOS dosimeters," *IEEE Trans. Nucl. Sci.*, vol. 41, no. 6, pp. 445-451, 1994.
- [11] L. Scheick, P. McNulty, D. Roth, B. Mason, and M. Davis., "Measurements of dose with individual FAMOS transistors," *IEEE Trans. Nucl. Sci.*, vol. 44, no. 6, pp. 1751-1756 1999.
- [12] E. S. Yang, *Electronic Devices*. MacGraw Hill: NY 1993.
- [13] W. Brown, *Nonvolatile Semiconductor Memory Technology*. IEEE Press, 1998.
- [14] A. Casarett, *Radiation Biology*. Prentice Hall: Englewood 1968.
- [15] D. Lea, *Actions of Radiation on Living Cells*. Cambridge Univ. Press: NY 1947.
- [16] T. P. Ma and P.V. Dressendorfer, *Ionizing Radiation Effects in MOS Devices and Circuits*, New York: John Wiley and Sons, 1989.
- [17] P. E. Dodd, O. Musseau, M. R. Shaneyfelt, F. W. Sexton, C. D'hose, G. L. Hash, M. Martinez, R. A. Loemker, J. L. Leray, and P. S. Winokur, "Impact of ion energy on single-event upset," *IEEE Trans. Nucl. Sci.*, vol. 45, no. 6, pp. 2483-2491, 1998.
- [18] J. L. Titus, C. F. Wheatley, K. M Van Tyne, J. F. Krieg, D. I. Burton, and A. B. Campbell, "Effect of ion energy upon dielectric breakdown of the capacitor response in vertical power MOSFETs," *IEEE Trans. Nucl. Sci.*, vol. 45, no. 6, pp. 2483-2499, 1998.
- [19] A. H. Johnston, G. M. Swift, T. Miyahira, and L. D. Edmonds, "Breakdown of gate oxides during irradiation with heavy ions," *IEEE Trans. Nucl. Sci.*, vol. 45, no. 6, pp. 2500-2508, 1998.
- [20] P. M. Lenehan and J. F. Conley, Jr., "A comprehensive physically based predictive model for radiation damage in MOS systems," *IEEE Trans. Nucl. Sci.*, vol. 45, no. 6, pp. 2413-2423, 1998.
- [21] F. Saigne, L. Dusseau, J. Fesquet, J. Gasiot, R. Ecoffet, J. David, R. Schrimpf, and K. Galloway, "Experimental validation of an accelerated method of oxide-trap-level characterization for predicting long term thermal effects in metal oxide semiconductor devices," *IEEE Trans. Nucl. Sci.*, vol. 44, no. 6, pp. 2001-2006, 1998.
- [22] O. Flament, J. Autran, P. Paillet, P. Roche, O. Faynot, and R. Truche, "Charge pumping analysis of radiation effects in locos parasitic transistors," *IEEE Trans. Nucl. Sci.*, vol. 44, no. 6, pp. 1930-1938, 1998.
- [23] R. Lawrence, B. Mrstik, H. Hughes, and P. McMarr, "Radiation induced charge in SIMOX buried oxides: lack of thickness dependence at low applied fields," *IEEE Trans. Nucl. Sci.*, vol. 44, no. 6, 2095-2100, 1998.
- [24] D. Fleetwood, M. Johnson, T. Meisenheimer, P. Winokur, W. Warren, and S. Witezak, "1/f noise, hydrogen transport and latent interface-trap buildup in irradiated MOS devices," *IEEE Trans. Nucl. Sci.*, vol. 44, no. 6, pp. 1810-1817, 1998.
- [25] AIP handbook, American Institute of Physics, 1995. p. 8-181.
- [26] G. Knoll, *Radiation Detection and Measurement*, NY: Wiley & Sons, Incorporated, 1990, pp. 44-50.
- [27] H. Johns and J. Cunningham. *The Physics of Radiology*. Charles Thomas: Springfield 1974, pp. 363-5.
- [28] L. Dusseau, G. Ranchoux, G. Polge, D. Plattard, F. Saigne, J. Bessiere, J. Fesquet, and J. Gasiot, "High energy electron dose-mapping using optically stimulated luminescent films," *IEEE Trans. Nucl. Sci.*, vol. 46, no. 6, pp. 1757-1761 1999.
- [29] International Commission on Radiation Units and Measurements, "Stopping powers for electrons and positrons," No. 37, p. 60.
- [30] International Commission on Radiation Units and Measurements, "Linear energy transfer," No. 16, p. 5.
- [31] J. Titus, C. Wheatley, K. Van Tyne, J. Krieg, D. Burton, and A. Campbell, "Effect of ion energy upon dielectric breakdown of the capacitor response in vertical power MOSFETs," *IEEE Trans. Nucl. Sci.*, vol. 46, no. 6, pp. 2492-2499, 1998.
- [32] P. McNulty, L. Scheick, and D. Roth, "First failure predictions for EPROMs of the type flown on the MPTB satellite," *IEEE Trans. Nucl. Sci.*, submitted for publication.